

Extreme learning machines for variance-based global sensitivity analysis *

John Darges[†], Alen Alexanderian[‡], and Pierre Gremaud[§]

Abstract. Variance-based global sensitivity analysis (GSA) can provide a wealth of information when applied to complex models. A well-known Achilles’ heel of this approach is its computational cost which often renders it unfeasible in practice. An appealing alternative is to analyze instead the sensitivity of a surrogate model with the goal of lowering computational costs while maintaining sufficient accuracy. Should a surrogate be “simple” enough to be amenable to the analytical calculations of its Sobol’ indices, the cost of GSA is essentially reduced to the construction of the surrogate. We propose a new class of sparse weight Extreme Learning Machines (SW-ELMs) which, when considered as surrogates in the context of GSA, admit analytical formulas for their Sobol’ indices and, unlike the standard ELMs, yield accurate approximations of these indices. The effectiveness of this approach is illustrated through both traditional benchmarks in the field and on a chemical reaction network.

Key words. Global sensitivity analysis, Sobol’ indices, neural networks, extreme learning machines, surrogate models, sparsification

AMS subject classifications. 65C20, 65C60, 65D15, 62H99 62J10

1. Introduction. A key insight into the behavior of a generic model of the form

$$(1.1) \quad y = f(\mathbf{x}), \quad \mathbf{x} \in \mathbb{R}^d, y \in \mathbb{R},$$

is to understand the impact of the uncertainty in the entries of $\mathbf{x} = (x_1, \dots, x_d)$ on the uncertainty in the model output y ; this can be addressed by performing global sensitivity analysis (GSA) [9, 10, 21]. We focus on variance based GSA [20, 22, 25] whereby one seeks to quantify the relative contributions of the entries of \mathbf{x} to the variance of f . Specifically, we rely on the Sobol’ indices [25] and assume that the entries of \mathbf{x} in (1.1) can be regarded as independent uniformly distributed random variables—which is common in applications.

Computing Sobol’ indices generally involves a costly sampling procedure and multiple applications of Monte Carlo integration. This is not feasible for applications where the function f is expensive to evaluate and/or the input dimension d is large. In such cases, a common approach is to construct a surrogate model $\hat{f} \approx f$ whose Sobol’ indices can be computed efficiently [3, 23]. A number of surrogate models have been proposed for this task, including polynomial chaos expansions (PCEs) [1, 26], multivariate adaptive regression splines (MARS) [2, 5], and Gaussian processes [11, 14, 17]. For a few surrogate models, it is possible to derive analytical expressions of their Sobol’ indices thereby essentially reducing the cost of GSA to the cost of constructing \hat{f} . PCE surrogates have this desirable property. Analytical formulas for the Sobol’ indices of Gaussian process surrogates have also been derived [11, 17].

*Submitted to the editors January 17, 2022.

Funding: Supported in part by US National Science Foundation grants DMS #1745654 and DMS #1953271.

[†]Department of Mathematics, North Carolina State University, Raleigh, NC, USA

[‡]Department of Mathematics, North Carolina State University, Raleigh, NC, USA

[§]Department of Mathematics and The Graduate School, North Carolina State University, Raleigh, NC, USA

In this article, we present an alternative approach which uses extreme learning machine (ELM) surrogates—a class of neural networks—for which Sobol’ indices can be computed analytically.

ELMs are a class of single layer neural networks [7, 8, 12] where, unlike traditional neural networks, one draws weights and biases of the hidden layer randomly. Consequently, training an ELM amounts to solving a linear least squares problem to estimate the output layer weights; see [section 2](#) for more details. Our motivation for considering ELMs for GSA is twofold

- they are simple and inexpensive to train: only a linear least squares problem needs to be solved,
- through a judicious choice of the activation function, analytic formulas for the Sobol’ indices can be derived; see [section 3](#).

The use of neural networks in uncertainty quantification has been the object of recent research efforts. Among many others, [13, 16, 28] have for instance used neural network surrogates for GSA. To our knowledge, however, the present work is the first of its kind to derive analytic formulas for Sobol’ indices of neural network surrogates.

To be used reliably for variance based GSA, the surrogate \hat{f} must capture some key structural properties of the exact model f . To illustrate this point, consider [\(1.1\)](#) with $\mathbf{x} \in \mathbb{R}^3$ and assume f has mean zero. The ANOVA decomposition of f is given by

$$(1.2) \quad f(x_1, x_2, x_3) = \sum_{i=1}^3 f_i(x_i) + f_{12}(x_1, x_2) + f_{13}(x_1, x_3) + f_{23}(x_2, x_3) + f_{123}(x_1, x_2, x_3),$$

where $f_i = \mathbb{E}(f|x_i)$, $f_{ij} = \mathbb{E}(f|x_i, x_j) - f_i - f_j$, and $f_{123} = f - \sum_{i=1}^3 f_i - \sum_{i<j} f_{ij}$. A key observation is that the variance of f can be decomposed as the sum of the variances of the individual terms in the ANOVA. This makes it possible to quantify the contributions of the individual inputs (or a group of inputs) to the total variance of f and leads to definition of Sobol’ indices. To provide accurate estimates of Sobol’ indices, a surrogate \hat{f} must emulate the main effect terms $\{f_i\}_{i=1}^d$ as well as the higher order interaction terms in [\(1.2\)](#). As discussed in [section 4](#), standard ELMs may fail to correctly capture the impact of variable interactions on output variance, leading to inaccurate Sobol’ indices. We resolve this shortcoming by introducing sparsity in the construction of an ELM which enhances the ability of the surrogate to emulate complex variable interactions. We demonstrate the efficiency of this approach on standard benchmark problems and on an application from biochemistry (see [section 5](#)).

2. Extreme learning machines. A single-layer neural network with n hidden layer neurons and a scalar output has the form

$$(2.1) \quad g(\mathbf{x}) = \sum_{j=1}^n \beta_j \phi(\mathbf{w}_j^\top \mathbf{x} + b_j),$$

where $\mathbf{w}_j \in \mathbb{R}^d$, $b_j \in \mathbb{R}$, $j = 1, \dots, n$, are the weights and biases of the hidden layer, β_j , $j = 1, \dots, n$, are the weights of the output layer, and ϕ is the hidden layer activation function. For a given number of neurons n and a given activation function ϕ , we set

$$(2.2) \quad \mathcal{M}_n(\phi) = \left\{ \sum_{j=1}^n \beta_j \phi(\mathbf{w}_j^\top \mathbf{x} + b_j); b_j, \beta_j \in \mathbb{R}, \mathbf{w}_j \in \mathbb{R}^d \right\}.$$

It is known that single-layer neural networks are dense in $\mathcal{C}(\mathbb{R}^d)$; more precisely, if $\phi \in \mathcal{C}(\mathbb{R})$ is not polynomial and $f \in \mathcal{C}(K)$ where K is a compact subset of \mathbb{R}^d then, for any $\epsilon > 0$, there exists n and $g_n \in \mathcal{M}_n(\phi)$ such that [19]

$$(2.3) \quad \max_{\mathbf{x} \in K} |f(\mathbf{x}) - g_n(\mathbf{x})| < \epsilon.$$

The standard approach to train (2.1) is to determine all hidden layer weights and biases and output weights by solving a nonlinear least-squares problem.

In an Extreme Learning Machine (ELM) [8], the weight vectors \mathbf{w}_j and biases b_j , $j = 1, \dots, n$, of the hidden layer are not determined as part of a regression process but rather are *chosen randomly*. Training an ELM then only involves determining the output layer weights $\{\beta_j\}_{j=1}^n$ by solving a *linear*-least squares problem. Remarkably, even though it bypasses training the hidden layer weights—and replaces a costly non-linear least-squares problem by a linear one—ELM retains the universal approximation property (2.3), provided the hidden layer weights and biases are sampled from a continuous probability distribution [6].

2.1. Computing ELM surrogates. Let $\mathbf{W} = [\mathbf{w}_1 \ \mathbf{w}_2 \ \dots \ \mathbf{w}_n]^\top$, $\mathbf{b} = [b_1 \ b_2 \ \dots \ b_n]^\top$, and $\boldsymbol{\beta} = [\beta_1 \ \beta_2 \ \dots \ \beta_n]^\top$; the ELM (2.1) takes the form

$$(2.4) \quad g(\mathbf{x}) = \boldsymbol{\beta}^\top \phi(\mathbf{W}\mathbf{x} + \mathbf{b}),$$

where ϕ is understood to act componentwise and the weight matrix \mathbf{W} and bias vector \mathbf{b} are sampled from a continuous probability distribution \mathcal{D} , i.e., $w_{j,l}, b_j \sim \mathcal{D}$, $j = 1, \dots, n$ and $l = 1, \dots, d$.

To construct a surrogate, the model f is sampled at $\{\mathbf{x}_i\}_{i=1}^m$, yielding $y_i = f(\mathbf{x}_i)$, $i = 1, \dots, m$. We then find $\boldsymbol{\beta}$ by solving

$$(2.5) \quad \min_{\boldsymbol{\beta} \in \mathbb{R}^n} \|\mathbf{H}\boldsymbol{\beta} - \mathbf{y}\|_2,$$

where $\mathbf{y} = [y_1 \ \dots \ y_m]^\top$ and $H_{ij} = \phi(\mathbf{w}_j^\top \mathbf{x}_i + b_j)$ for $i, j \in \{1, \dots, m\} \times \{1, \dots, n\}$.

In our computations, we implement a regularized least squares problem to control the magnitude of the solution $\boldsymbol{\beta}$:

$$(2.6) \quad \min_{\boldsymbol{\beta}} \frac{1}{2} \|\mathbf{H}\boldsymbol{\beta} - \mathbf{y}\|_2^2 + \frac{\alpha}{2} \|\boldsymbol{\beta}\|_2^2,$$

with $\alpha > 0$, the solution of which is

$$\boldsymbol{\beta}^* = (\mathbf{H}^\top \mathbf{H} + \alpha \mathbf{I})^{-1} \mathbf{H}^\top \mathbf{y}.$$

The regularization parameter α can be selected using the L-curve method or generalized cross validation (GCV) [4]. We construct the hidden layer weight matrix and bias vector by sampling individual values from the standard normal distribution and use Latin hypercube sampling (LHS) to sample points in the training set $\{\mathbf{x}_i\}_{i=1}^m$.

3. Global sensitivity analysis using ELMs. For each entry x_k , $k = 1, \dots, d$, the first order Sobol' index S_k and total Sobol' index S_k^{tot} of a surrogate $y = \hat{f}(\mathbf{x})$ are defined as

$$(3.1) \quad S_k = \frac{\text{var}(\hat{f}_k)}{\text{var}(\hat{f})}, \quad S_k^{\text{tot}} = 1 - \frac{\text{var}(\mathbb{E}(\hat{f}|x_l, l \neq k))}{\text{var}(\hat{f})},$$

where $\hat{f}_k(x_k) = \mathbb{E}(\hat{f}|x_k) - \mathbb{E}(\hat{f})$; see e.g., [20]. Henceforth, we assume that the entries of the input vector \mathbf{x} are independent and uniformly distributed on the interval $[0, 1]$ and, therefore, the input domain is $[0, 1]^d$. It is straightforward to extend the proposed approach to the case where entries of \mathbf{x} are independent uniformly distributed random variables on arbitrary closed and bounded intervals.

To obtain analytic formulas for the Sobol' indices while avoiding Monte Carlo approximations, we must be able to easily compute the mean, variance, and partial variances of the surrogate. By carefully choosing the activation function, we can design \hat{f} as an ELM which (i) suits the above requirement and (ii) preserves the universal approximation property. Activation functions traditionally used in machine learning are not suited for our purpose as the corresponding calculations in (3.1) become impractical or impossible. Instead, we choose an exponential activation function

$$\phi(t) = e^t,$$

which results in

$$(3.2) \quad \hat{f}(\mathbf{x}) = \sum_{j=1}^n \beta_j e^{\mathbf{w}_j^\top \mathbf{x} + b_j} = \sum_{j=1}^n \left(\beta_j e^{b_j} \prod_{l=1}^d e^{w_{j,l} x_l} \right).$$

Since ϕ a smooth non-polynomial function, the results cited in section 2 apply and ELMs constructed this way still have the universal approximation property.

We now compute the first and second moments of (3.2).

Lemma 3.1. *The mean and variance of the ELM (3.2) are*

$$\mathbb{E}(\hat{f}) = \sum_{j=1}^n \left(\beta_j e^{b_j} \prod_{l=1}^d \epsilon(w_{j,l}) \right)$$

and

$$\text{var}(\hat{f}) = \sum_{j,i=1}^n \beta_j \beta_i e^{b_j + b_i} \left(\prod_{l=1}^d \epsilon(w_{j,l} + w_{i,l}) - \prod_{r=1}^d \epsilon(w_{j,r}) \epsilon(w_{i,r}) \right),$$

$$\text{where } \epsilon(t) = \begin{cases} \frac{e^t - 1}{t}, & t \neq 0 \\ 1, & t = 0 \end{cases}$$

Proof. See Appendix A. ■

Using Lemma 3.1, we obtain analytic expressions for the Sobol' indices of (3.2).

Proposition 3.2. *The first and total order Sobol' indices of the ELM (3.2) are given by*

$$(3.3) \quad S_k = \frac{1}{\text{var}(\hat{f})} \sum_{j,i=1}^n \beta_j \beta_i e^{b_j + b_i} (\epsilon(w_{j,k} + w_{i,k}) - \epsilon(w_{j,k})\epsilon(w_{i,k})) \prod_{l \neq k} \epsilon(w_{j,l})\epsilon(w_{i,l})$$

and

$$(3.4) \quad S_k^{\text{tot}} = 1 - \frac{1}{\text{var}(\hat{f})} \sum_{j,i=1}^n \beta_j \beta_i e^{b_j + b_i} \epsilon(w_{j,k})\epsilon(w_{i,k}) \left(\prod_{r \neq k} \epsilon(w_{j,r} + w_{i,r}) - \prod_{l \neq k} \epsilon(w_{j,r})\epsilon(w_{i,l}) \right),$$

respectively, for $k = 1, \dots, d$.

Proof. See [Appendix A](#). ■

4. Sparse ELMs. ELM surrogates (2.4) are constructed by randomly sampling the hidden layer weight matrix \mathbf{W} and bias vector \mathbf{b} from the standard normal distribution. As pointed out in [Section 2](#), an ELM surrogate \hat{f} can be found to satisfy

$$(4.1) \quad \hat{f} \approx f$$

as accurately as desired. Our goal is however not so much to construct \hat{f} satisfying (4.1) within a given tolerance but rather to construct \hat{f} such that

$$(4.2) \quad S(\hat{f}) \approx S(f),$$

where S stands here for any of the Sobol' indices from [Proposition 3.2](#) and $S(\hat{f})$ can be computed at low cost. To ensure that the Sobol' indices computed from \hat{f} yield a reliable description of the variable interactions, we thus have to construct a surrogate \hat{f} that not only satisfies (4.1) but also

$$(4.3) \quad \hat{f}_u \approx f_u, \quad \text{for any } u \subset \{1, \dots, d\},$$

where f_u and \hat{f}_u are the terms corresponding to the subset u in the ANOVA decomposition of f and \hat{f} respectively.

4.1. ELMs and variable interactions. Simple examples show that the amount of variable interactions in f plays a key role in either achieving or failing to achieve (4.2). As an illustration, consider the following parametrized function

$$(4.4) \quad f_\delta(\mathbf{x}) = \sum_{i=1}^d x_i + \delta \prod_{j=1}^d (1 + x_j), \quad \mathbf{x} \in [0, 1]^d,$$

where δ controls the amount of variable interactions. When $\delta = 0$, f_δ is fully additive: there is no variable interactions and thus the first order and corresponding total Sobol indices are equal. For $\delta > 0$, there is interaction between the variables in increasing amount with increasing values of δ . By construction, we also observe that the individual entries x_i , $i = 1, \dots, d$, all share the same Sobol' indices; this feature is not present when considering the ELM

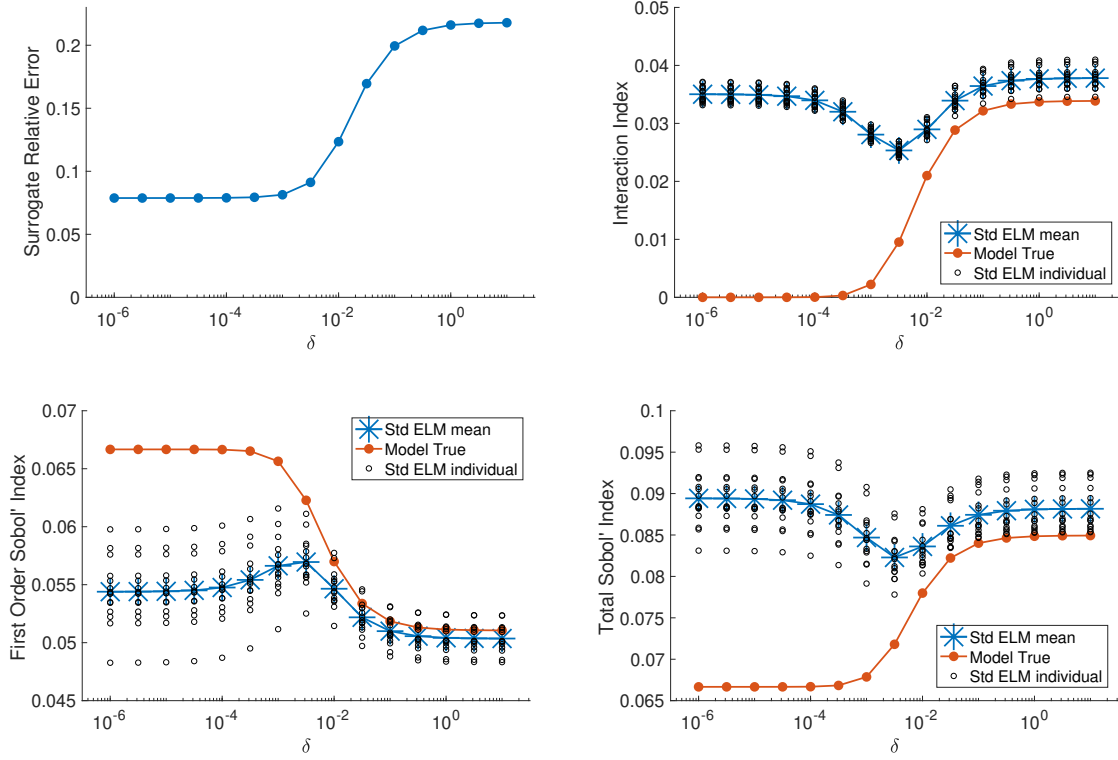


Figure 1. Example (4.4) with $d = 15$. Top left: Surrogate relative error; bottom left: first order Sobol' indices $S_i(f)$ and $S_i(\hat{f})$ of x_i , $i = 1, \dots, 15$ and corresponding mean; bottom right: total Sobol' indices $S_i^{\text{tot}}(f)$ and $S_i^{\text{tot}}(\hat{f})$ of x_i , $i = 1, \dots, 15$, and corresponding mean; top right: interaction indices $I_i := S_i^{\text{tot}} - S_i$, $i = 1, \dots, 15$, for both f and \hat{f} .

surrogate \hat{f} instead of f because of approximation errors. The first order and total Sobol' indices of (4.4) can be found analytically and are given in Appendix B. Therefore, by varying δ , we can explore how variable interactions affect accuracy in both (4.1) and (4.2).

To approximate the Sobol' indices of (4.4) with $d = 15$, we construct ELMs of the form (3.2) as follows:

- 1: collect $m = 900$ training points sampled by LHS
- 2: construct ELMs with $n = 300$ neurons
- 3: compute the surrogate relative error

$$E_{\text{surr}} = \frac{1}{\sqrt{\sum_{j=1}^s y_j^2}} \sqrt{\sum_{j=1}^s (\hat{f}(\mathbf{x}_j) - y_j)^2}, \quad y_j = f(\mathbf{x}_j) \quad j = 1, \dots, s,$$

using $s = 1000$ validation points sampled by LHS

- 4: select a regularization parameter $\alpha = 10^{-3}$ by the L-curve method
- 5: compute Sobol' indices of the ELM surrogate using (3.3) and (3.4)

Figure 1 (top left) illustrates that, unsurprisingly, the surrogate relative error—which

measures the discrepancy in (4.1)—increases as the amount of interactions increases with δ . Interestingly, the situation is reversed when looking at the accuracy of the Sobol' indices through (4.2). Indeed, Figure 1 (bottom left) shows that while for any i , $i = 1, \dots, d$, $S_i(\hat{f})$ is a close approximation of $S_i(f)$ for the larger values of δ , the relative accuracy of the corresponding approximations decreases for smaller levels of interaction (i.e., smaller values of δ). The variance of the $S_i(\hat{f})$'s, which again should ideally all have the value $S_1(f) = \dots = S_d(f)$, also increases with smaller values of δ . The total Sobol' indices and their approximations largely behave in similar fashion, see Figure 1 (bottom right). This example shows that ELM based surrogates have a tendency to overestimate variable interactions, a point made clear in Figure 1 (top right) where the interaction indices $I_i := S_i^{\text{tot}} - S_i$, $i = 1, \dots, d$ are considered.

These results demonstrate that, for variance based GSA, standard ELM may fail to effectively adapt when applied to models featuring different degrees of contribution from interaction terms to the output variance.

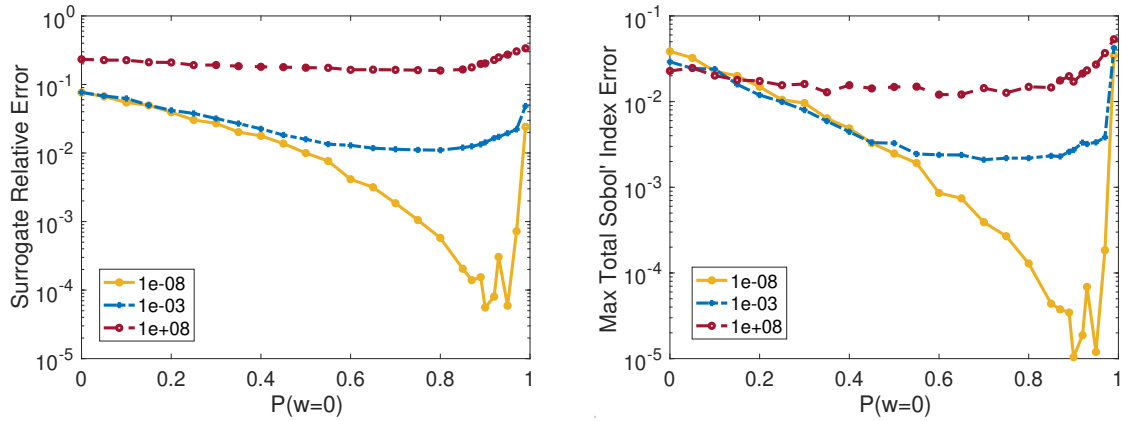


Figure 2. Example (4.4) with $d = 15$, with low variable interactions $\delta = 10^{-8}$, limited variable interactions 10^{-3} , and strong variable interactions 10^8 . Surrogate relative error (left) and largest absolute error in total Sobol' index approximation (right).

4.2. Hidden layer weight sparsification. We propose sparsifying the hidden layer weight matrix \mathbf{W} before training the output weights as a means of controlling the influence of variable interactions. Specifically, we replace \mathbf{W} by a sparse weight matrix $\widetilde{\mathbf{W}}$ defined as

$$(4.5) \quad \widetilde{\mathbf{W}} = \mathbf{B} \circ \mathbf{W},$$

where \mathbf{B} is a $n \times d$ -matrix with independent Bernoulli entries, i.e.,

$$(4.6) \quad B_{ij} = \begin{cases} 0 & \text{with probability } p, \\ 1 & \text{with probability } 1 - p \end{cases},$$

and where \circ stands for the elementwise matrix multiplication. The sparsification parameter $p \in [0, 1)$ determines how sparse the hidden layer weight matrix is. If $p = 0$, then $\widetilde{\mathbf{W}} = \mathbf{W}$

and the method reverts to standard ELM; when p is selected to be near 1, the weight matrix $\widetilde{\mathbf{W}}$ is sparse. This technique strays from the ELM theory which assumes sampling weights from a continuous probability distribution to guarantee universal approximation.

We implement the sparse weight ELM (SW-ELM) approach, i.e., ELM with $\widetilde{\mathbf{W}}$ instead of \mathbf{W} as a hidden layer weight matrix, on example (4.4). Figure 2 illustrates the results for a range of values of the sparsification parameter p and for three values of δ corresponding to low variable interactions ($\delta = 10^{-8}$), limited variable interactions ($\delta = 10^{-3}$), and strong variable interactions ($\delta = 10^8$). In the case of low variable interactions ($\delta = 10^{-8}$), Figure 2 shows that using a sparse weight matrix can dramatically increase the accuracy of both the ELM surrogate and of the Sobol' indices computed using that surrogate. Sparsifying the weight matrix may thus lead to significant improvements in GSA results when dealing with models with low interaction terms. On the other hand, in cases where interaction terms are prominent in the model, sparsifying the hidden layer weight matrix may offer no improvement or may even result in loss of accuracy.

4.3. Selection of sparsification parameter. Figure 2 suggests a framework for how to implement SW-ELM for a given model; indeed, for fixed values of δ and varying values of p , we observe similar trends in the surrogate error and in the total Sobol' index approximation error. This indicates that we may use the surrogate error as a guideline when searching for the best sparsification parameter.

We propose creating a validation set alongside the training set when using SW-ELM surrogates for GSA. Subsequently, we select r values of the sparsification parameter p and construct corresponding sparse weight matrices. Then, ELMs are trained using each weight matrix and the validation set is used to compute the surrogate error for each ELM. This serves as a diagnostic tool to aid in deciding whether sparsification may improve Sobol' index approximation. If sparsification yields an improved surrogate error, then we use the SW-ELM with the lowest surrogate error to approximate Sobol' indices. If, on the other hand, sparsification does not yield a notable improvement then we may default to using standard ELM. We summarize the method in Algorithm 4.1.

We illustrate the power of this method by repeating the experiment in Figure 1 for (4.4) using SW-ELM instead of ELM. Figure 3 displays the total Sobol' indices for both surrogates as well as the exact indices. SW-ELM displays increased accuracy and reduced variance across all tested ranges of interaction strength.

In the context of GSA, SW-ELM displays better accuracy and flexibility than standard ELM. The proposed implementation is only marginally more costly than standard ELM as there is no need to re-sample training or validation points for each ELM.

5. Computational results.

5.1. Analytic example: Sobol' g-function. The Sobol' g-function [22]

$$(5.1) \quad f(\mathbf{x}) = \prod_{i=1}^d g_i(x_i) \quad \mathbf{x} \in [0, 1]^d, \quad g_i(x_i) = \frac{|4x_i - 2| + a_i}{1 + a_i}, \quad i = 1, \dots, d,$$

is commonly used as a benchmark to test new methods; its nonlinearity and lack of smoothness make approximating its Sobol' indices a significant challenge. The constants a_i , chosen

Algorithm 4.1 GSA with sparse weight ELM

Input: (i) Model f ; (ii) training set $\{\mathbf{x}_i, y_i\}_{i=1}^m$; (iii) validation set $\{\mathbf{x}'_j, y'_j\}_{j=1}^s$; (iv) number of neurons n ; (v) candidate sparsification values $\{p_l\}_{l=1}^r$ (with $p_1 = 0$)

Output: (i) First order Sobol' indices $\{S_k\}_{k=1}^n$ and (ii) total Sobol' indices $\{S_k^{\text{tot}}\}_{k=1}^n$

- 1: Generate weight matrix \mathbf{W}_0 and bias vector \mathbf{b} using a standard normal distribution
- 2: **for** $l = 1, \dots, r$ **do**
- 3: Construct $\mathbf{W}_l = \mathbf{B} \circ \mathbf{W}_0$ with \mathbf{B} from (4.6) with $p = p_l$
- 4: Determine regularization parameter α_l by the L-curve method
- 5: Find output weights β_l by training ELM using $\mathbf{W}_l, \mathbf{b}, \alpha_l$ (see (2.6))
- 6: Compute relative surrogate error E_l
- 7: **end for**
- 8: Select hidden layer weight matrix \mathbf{W} and output weights β corresponding to sparsification parameter that gives smallest relative surrogate error
- 9: With \mathbf{W}, β , and \mathbf{b} , compute first order Sobol' indices $\{S_k\}_{k=1}^n$ and total Sobol' indices $\{S_k^{\text{tot}}\}_{k=1}^n$ using (3.3) and (3.4), respectively

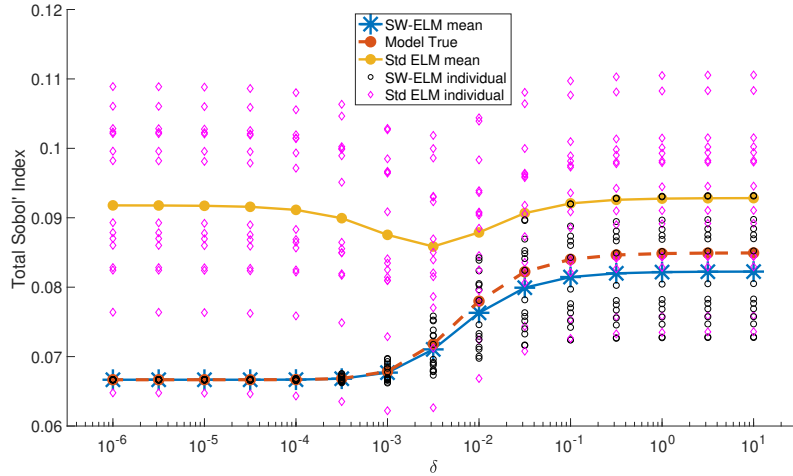


Figure 3. Example (4.4) true analytic total Sobol' indices compared to those approximated by standard ELM and sparse weight ELM (SW-ELM). All approximated indices are plotted along with means for each δ .

from the interval $(-1, \infty)$, can be tuned to determine which input variables are important. The closer a_i is to -1 the more "important" x_i becomes. On the other hand, the relative importance of x_i diminishes with larger values of a_i . For our test, we take the input dimension $d = 8$ and let $\mathbf{a} = [1, 2, 5, 10, 20, 50, 100, 500]$ as in [26].

We train our SW-ELM surrogates with 160 hidden layer neurons using 400 training points and 100 validation points, all sampled by Latin hypercube sampling (LHS). The regularization parameter $\alpha = 10^{-3}$ is selected by the L-curve method. The sparsification parameter p is determined through Algorithm (4.1). While Figure 4 does not show drastic improvements in error, we nevertheless conclude from this test that sparsifying may improve our approximations

when performing GSA; we select the sparsification parameter $p = 0.85$.

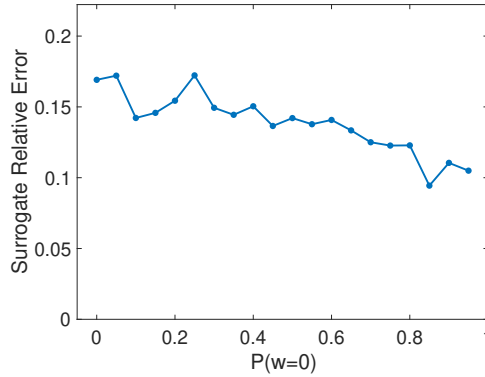


Figure 4. Sparsification test for 8-dimensional g -function (5.1) with $\mathbf{a} = [1, 2, 5, 10, 20, 50, 100, 500]$. Relative surrogate error is estimated using validation set with 100 points.

As can be seen from Figure 5, SW-ELM correctly ranks the Sobol' indices and successfully identifies the most influential input variables. For important input variables, each approximated first order Sobol' index is within 5% relative error of the respective true first order Sobol' index while each approximated total Sobol' index is within 7% relative error of the respective true total Sobol' index.

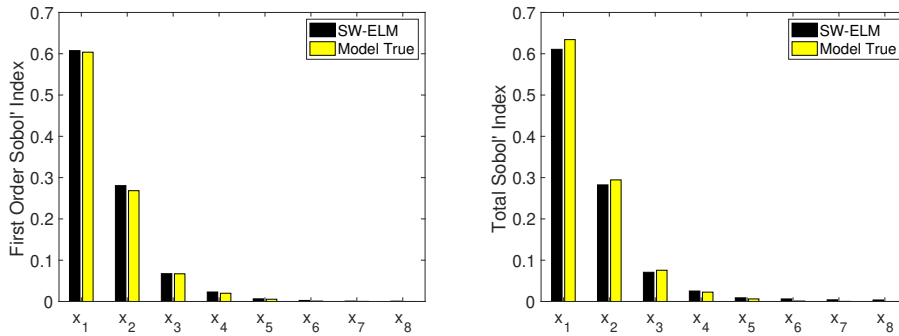


Figure 5. 8-dimensional g -function (5.1) with $\mathbf{a} = [1, 2, 5, 10, 20, 50, 100, 500]$. First order (left) and total (right) Sobol' indices approximated via SW-ELM and computed analytically.

5.2. Genetic oscillator. We examine the performance of the proposed approach on a challenging application problem from biochemistry, specifically, the genetic oscillator system which describes the time evolution of molecular species involved in the regulation of circadian rhythm [27]. The reaction network consists of sixteen reactions and involves nine species. The reactions, the corresponding propensity functions, and the nominal values of the rate parameters are given in Table 1. We consider the reaction rate equations (RREs), described by a nonlinear system of ordinary differential equations (ODEs), for this reaction network; see e.g., [27], [24], or [15], which we follow in the specific problem formulation used in the present

Reaction	Propensity Function	Parameter	Value
$P_a \rightarrow P_a + mRNA_a$	$\alpha_A P_a$	α_A	50.0
$P_r \rightarrow P_r + mRNAr$	$\alpha_R P_r$	α_R	0.01
$mRNA_a \rightarrow mRNA_a + A$	$\beta_A mRNA_a$	β_A	50.0
$mRNAr \rightarrow mRNAr + R$	$\beta_R mRNAr$	β_R	5.0
$A + R \rightarrow C$	$\gamma_C AR$	γ_C	20.0
$P_a + A \rightarrow P_{a-A}$	$\gamma_A P_a A$	γ_A	1.0
$P_{a-A} \rightarrow P_a + A$	$\theta_A P_{a-A}$	θ_A	50.0
$P_r + A \rightarrow P_{r-A}$	$\gamma_R P_r A$	γ_R	1.0
$P_{r-A} \rightarrow P_r + A$	$\theta_R P_{r-A}$	θ_R	1.0
$A \rightarrow \emptyset$	$\delta_A A$	δ_A	1.0
$R \rightarrow \emptyset$	$\delta_R R$	δ_R	0.2
$mRNA_a \rightarrow \emptyset$	$\delta_{MA} mRNA_a$	δ_{MA}	10.0
$mRNAr \rightarrow \emptyset$	$\delta_{MR} mRNAr$	δ_{MR}	0.5
$C \rightarrow R$	$\delta'_A C$	δ'_A	1.0
$P_{a-A} \rightarrow P_{a-A} + mRNA_a$	$\alpha_a \alpha_A P_{a-A}$	α_a	10.0
$P_{r-A} \rightarrow P_{r-A} + mRNAr$	$\alpha_r \alpha_R P_{r-A}$	α_r	5000

Table 1

Genetic oscillator reactions, propensity functions, parameters and nominal values of the parameters [15, 24].

study. We focus on the uncertainty in the reaction rate parameters. A uniform distribution is attached to each rate parameter on an interval given by a $\pm 5\%$ perturbation from the corresponding nominal value. We use a random vector $\mathbf{x} \in \mathbb{R}^{16}$, whose entries are uniformly distributed on $[0, 1]$, to parameterize the uncertainty in the reaction rates. The vector of reaction rates is obtained by applying a linear transformation to \mathbf{x} that maps the entries of \mathbf{x} to the respective physical ranges. In the present study, we consider the quantity of interest (QoI) given by

$$(5.2) \quad f(\mathbf{x}) = \frac{1}{T} \int_0^T R(t; \mathbf{x}) dt,$$

where $R(t; \mathbf{x})$ is the concentration of the species R present in the system at time t , and T is the final simulation time. Notice that computing $R(t; \mathbf{x})$, for $t \in [0, T]$, requires solving the system of RREs with the reaction rates set according to \mathbf{x} . This system, for the present application, is given by a stiff system of nonlinear ODEs. Thus, evaluations of the QoI in (5.2) are computationally expensive.

Figure 6 (top row) presents approximations for first order and total Sobol' indices when using standard ELM. The experiment uses 3000 training points and 1000 neurons. The regularization parameter $\alpha = 10^{-4}$ is selected by the L-curve method. We observe that approximation using standard ELM leads to overestimations, particularly for unimportant input

variables, of the total Sobol' indices and underestimations of the first order Sobol' indices; this is a clear case of standard ELM overestimating contributions to the output variance by higher order interactions.

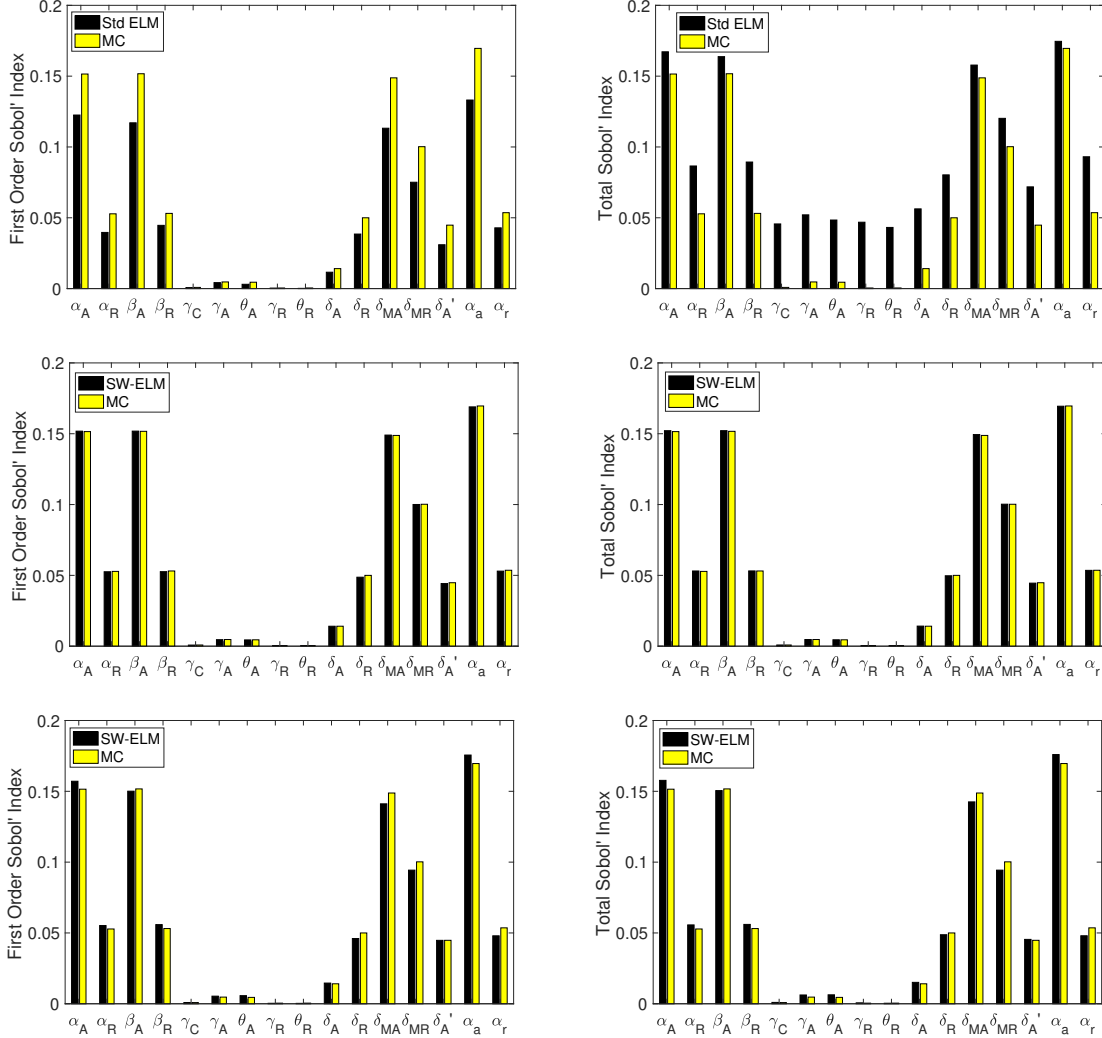


Figure 6. Top row: first order (left) and total Sobol's (right) indices corresponding to the QoI (5.2) approximated via standard ELM, using training set with 3000 points, along with those approximated via Monte Carlo using 10^6 sample points. Middle row: same experiment with SW-ELM, with 100 point validation set, instead of standard ELM. Bottom row: same experiment with SW-ELM instead of ELM and training size of 150 instead of 3000.

Let us instead tackle this problem using SW-ELM; we train our surrogates with again 3000 training points, using 1000 hidden layer neurons, and 100 validation points, all sampled by LHS. Regarding sparsification, we follow [Algorithm 4.1](#). The results of these tests are displayed in [Figure 7](#) (left), and show that as the hidden layer weight matrix become more sparse, the error in the surrogate improves dramatically; we select the sparsification parameter $p = 0.8$.

Figure 6 (middle row), displays the resulting approximated Sobol' indices and compares with the Sobol' indices approximated by Monte Carlo methods with 10^6 sample points. Given that the Sobol' indices computed via Monte Carlo methods are a close representation of the true Sobol' indices, SW-ELM provides an accurate approximation of the indices.

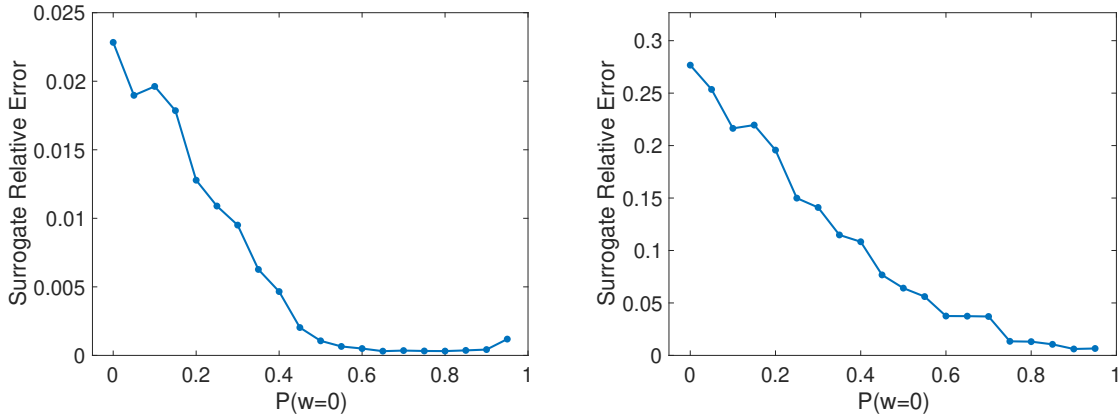


Figure 7. Sparsification test for 16-dimensional QoI (5.2). Left: ELMs trained with training size 3000. Right: ELMs trained with training size 150. Relative surrogate error is estimated using validation set with 100 points.

We can test the performance of SW-ELM further still. We train surrogates with only 150 training points, using 50 hidden layer neurons, and 100 validation points. The results of sparsification tests are displayed in Figure 7 (right). We select the sparsification parameter $p = 0.9$. Figure 6 (bottom row) displays the resulting approximated Sobol' indices. SW-ELM with 150 training points or 3000 training points gives very similar results. This indicates that SW-ELM is extremely efficient for this problem—a modest number of training samples are sufficient for obtaining accurate sensitivity analysis results.

As shown in Figure 6, the first order Sobol' indices and the total Sobol' indices are very close to each other for this application. This suggests that there are few, if any, higher order variable interactions present in the QoI function (5.2). The fact that the sparsity of the weight matrix had a significant influence over the quality of the ELM surrogate, as seen in Figure 7, further supports this. Here sparsification is not simply helpful; it is essential and allows us to drastically decrease the number of sample points needed to obtain accurate approximations.

6. Conclusion. The use of SW-ELM as a surrogate in the context of variance based GSA allows the user to completely eschew Monte Carlo integration which is a perennial bottleneck in this field. The numerical results we present above make a strong case for further study of the approach. In particular, there is in general very little known theoretically regarding the link from (4.1) (accurate surrogate) to (4.2) (accurate GSA). In our particular case, we note further that SW-ELM is not strictly covered by the existing theory [8] as the distribution we use for \mathbf{W} is not continuous.

A key point in our approach is the ability to analytically compute the Sobol' indices of \hat{f} . This is where the assumption of independent uniformly distributed parameters is crucial.

Further work will reveal to what extent this assumption might be weakened. A deeper understanding of the proposed sparsification process might also result in further improvement of the proposed approach.

References.

- [1] T. Crestaux, O. L. Maitre, and J.-M. Martinez. Polynomial chaos expansion for sensitivity analysis. *Reliability Engineering & System Safety*, 94(7):1161 – 1172, 2009. Special Issue on Sensitivity Analysis.
- [2] J. H. Friedman. Multivariate adaptive regression splines. *The Annals of Statistics*, 19(1):1–141, 1991. With discussion and a rejoinder by the author.
- [3] L. L. Gratiet, S. Marelli, and B. Sudret. Metamodel-based sensitivity analysis: polynomial chaos expansions and gaussian processes. In R. Ghanem, D. Higdon, and H. Owhadi, editors, *Handbook of Uncertainty Quantification*. Springer, 2017.
- [4] P. C. Hansen. *Getting Serious: Choosing the Regularization Parameter*, chapter 5, pages 85–107. Society for Industrial and Applied Mathematics, 2010.
- [5] J. Hart, A. Alexanderian, and P. Gremaud. Efficient computation of sobol’ indices for stochastic models. *SIAM Journal on Scientific Computing.*, 39(4):A1514–A1530, 2017.
- [6] G.-B. Huang and L. Chen. Convex incremental extreme learning machine. *Neurocomputing*, 70(16):3056–3062, 2007. Neural Network Applications in Electrical Engineering Selected papers from the 3rd International Work-Conference on Artificial Neural Networks (IWANN 2005).
- [7] G.-B. Huang, D. Wang, and Y. Lan. Extreme learning machines: a survey. *International Journal of Machine Learning and Cybernetics*, 2(2):107–122, 2011.
- [8] G.-B. Huang, Q.-Y. Zhu, and C.-K. Siew. Extreme learning machine: Theory and applications. *Neurocomputing*, 70(1):489–501, 2006. Neural Networks.
- [9] B. Iooss and P. Lemaître. *A Review on Global Sensitivity Analysis Methods*, pages 101–122. Springer US, Boston, MA, 2015.
- [10] B. Iooss and A. Saltelli. Introduction to sensitivity analysis. In R. Ghanem, D. Higdon, and H. Owhadi, editors, *Handbook of uncertainty quantification*, pages 1103–1122. Springer, 2017.
- [11] R. Jin, W. Chen, and A. Sudjianto. Analytical metamodel-based global sensitivity analysis and uncertainty propagation for robust design. *SAE transactions*, pages 121–128, 2004.
- [12] P. Jorgensen and D. E. Stewart. Approximation properties of ridge functions and extreme learning machines. *SIAM Journal on Mathematics of Data Science*, 3(3):815–832, 2021.
- [13] S. Li, B. Yang, and F. Qi. Accelerate global sensitivity analysis using artificial neural network algorithm: Case studies for combustion kinetic model. *Combustion and Flame*, 168:53–64, 2016.
- [14] A. Marrel, B. Iooss, B. Laurent, and O. Roustant. Calculations of sobol indices for the gaussian process metamodel. *Reliability Engineering & System Safety*, 94(3):742–751, 2009.
- [15] M. Merritt, A. Alexanderian, and P. A. Gremaud. Multiscale global sensitivity analysis for stochastic chemical systems. *Multiscale Modeling & Simulation*, 19(1):440–459, 2021.
- [16] J. Nagawkar and L. Leifsson. Efficient Global Sensitivity Analysis of Model-Based Ultrasonic Nondestructive Testing Systems Using Machine Learning and Sobol’ Indices.

- Journal of Nondestructive Evaluation, Diagnostics and Prognostics of Engineering Systems*, 4(4), 2021.
- [17] J. E. Oakley and A. O’Hagan. Probabilistic sensitivity analysis of complex models: a bayesian approach. *Journal of the Royal Statistical Society: Series B (Statistical Methodology)*, 66(3):751–769, 2004.
- [18] A. B. Owen. *Monte Carlo theory, methods and examples*. Art B. Owen, 2013.
- [19] A. Pinkus. Approximation theory of the mlp model in neural networks. *Acta Numerica*, 8:143–195, 1999.
- [20] C. Prieur and S. Tarantola. Variance-based sensitivity analysis: Theory and estimation algorithms. In R. Ghanem, D. Higdon, and H. Owhadi, editors, *Handbook of Uncertainty Quantification*, pages 1217–1239. Springer, 2017.
- [21] A. Saltelli, M. Ratto, T. Andres, F. Campolongo, J. Cariboni, D. Gatelli, M. Saisana, and S. Tarantola. *Global sensitivity analysis: the primer*. John Wiley & Sons, 2008.
- [22] A. Saltelli and I. Sobol’. Sensitivity analysis for nonlinear mathematical models: numerical experience. *Matematicheskoe Modelirovanie*, 7(11):16–28, 1995.
- [23] K. Sargsyan. Surrogate models for uncertainty propagation and sensitivity analysis. In R. Ghanem, D. Higdon, and H. Owhadi, editors, *Handbook of uncertainty quantification*. Springer, 2017.
- [24] P. W. Sheppard, M. Rathinam, and M. Khammash. A pathwise derivative approach to the computation of parameter sensitivities in discrete stochastic chemical systems. *The Journal of Chemical Physics*, 136(3):034115, 2012.
- [25] I. Sobol. Global sensitivity indices for nonlinear mathematical models and their Monte Carlo estimates. *Mathematics and Computers in Simulation*, 55(1–3):271–280, 2001. The Second IMACS Seminar on Monte Carlo Methods.
- [26] B. Sudret. Global sensitivity analysis using polynomial chaos expansions. *Reliability Engineering & System Safety*, 93(7):964–979, 2008. Bayesian Networks in Dependability.
- [27] J. M. Vilar, H. Y. Kueh, N. Barkai, and S. Leibler. Mechanisms of noise-resistance in genetic oscillators. *Proceedings of the National Academy of Sciences*, 99(9):5988–5992, 2002.
- [28] J. Walzberg, A. Carpenter, and G. A. Heath. Role of the social factors in success of solar photovoltaic reuse and recycle programmes. *Nature Energy*, 6(9):913–924, 2021.

Appendix A. Derivation of analytic formulas for ELM surrogate.

A.1. Proof of Lemma 3.1.

Proof. For the surrogate presented in this paper, we will derive expressions for the mean and variance. Recall the expression for the ELM (3.2) and the definition of the function $\epsilon(t)$, given in the statement of the lemma,

$$\epsilon(t) := \int_0^1 e^{tx} dx = \begin{cases} \frac{e^t - 1}{t} & t \neq 0, \\ 1 & t = 0. \end{cases}$$

We first find the expression for the mean:

$$\mathbb{E}(\hat{f}) = \int_{[0,1]^d} \sum_{j=1}^n \left(\beta_j e^{b_j} \prod_{l=1}^d e^{w_{j,l} x_l} \right) dx = \sum_{j=1}^n \left(\beta_j e^{b_j} \prod_{l=1}^d \int_0^1 e^{w_{j,l} x_l} dx_l \right).$$

Therefore, the mean can be expressed as

$$\mathbb{E}(\hat{f}) = \sum_{j=1}^n \left(\beta_j e^{b_j} \prod_{l=1}^d \epsilon(w_{j,l}) \right).$$

Next, we find the expression for the variance:

$$\begin{aligned} \text{var}(\hat{f}) &= \mathbb{E}(\hat{f}^2) - \mathbb{E}(\hat{f})^2 = \int_{[0,1]^d} \left(\sum_{j=1}^n (\beta_j e^{b_j} \prod_{l=1}^d e^{w_{j,l}x_l}) \right)^2 d\mathbf{x} - \mathbb{E}(\hat{f})^2 \\ &= \sum_{j,i=1}^n \left(\beta_j \beta_i e^{b_j+b_i} \prod_{l=1}^d \epsilon(w_{j,l} + w_{i,l}) \right) - \mathbb{E}(\hat{f})^2 \\ &= \sum_{j,i=1}^n \beta_j \beta_i e^{b_j+b_i} \left(\prod_{l=1}^d \epsilon(w_{j,l} + w_{i,l}) - \prod_{r=1}^d \epsilon(w_{j,r}) \epsilon(w_{i,r}) \right). \end{aligned} \quad \blacksquare$$

A.2. Proof of Proposition 3.2.

Proof. For the surrogate presented in this paper, we will derive expressions for the general formulas for regular and total Sobol' indices and offer simplified expressions for indices corresponding to single variables. Recall the expression for the ELM (3.2) and the function $\epsilon(t)$, and let $\mathbb{E}(\hat{f})$ and $\text{var}(\hat{f})$ be as presented in Lemma 3.1.

Given subset of variables of $\{x_1, \dots, x_d\}$, we first derive the expressions for Sobol' indices,

$$S_{\mathbf{u}} = \frac{\text{var}(\hat{f}_{\mathbf{u}})}{\text{var}(\hat{f})}, \quad \hat{f}_{\mathbf{u}} := \sum_{\mathbf{v} \subseteq \mathbf{u}} (-1)^{|\mathbf{u}|-|\mathbf{v}|} \mathbb{E}(\hat{f}|x_l, l \in \mathbf{v}),$$

where $\mathbf{u} \subset \{1, \dots, d\}$ [20]. Since terms in the ANOVA decomposition have the property that $\text{var}(\hat{f}_{\mathbf{u}}) = \mathbb{E}(\hat{f}_{\mathbf{u}}^2)$ [18] we can express the Sobol' index $S_{\mathbf{u}}$ for (3.2) as

$$\begin{aligned} S_{\mathbf{u}} &= \frac{\text{var}(\hat{f}_{\mathbf{u}})}{\text{var}(\hat{f})} = \frac{\mathbb{E}(\hat{f}_{\mathbf{u}}^2)}{\text{var}(\hat{f})} \\ &= \frac{1}{\text{var}(\hat{f})} \int_{[0,1]^d} \left(\sum_{\mathbf{v} \subseteq \mathbf{u}} \sum_{j=1}^n (-1)^{|\mathbf{u}|-|\mathbf{v}|} \beta_j e^{b_j} \left(\prod_{l \in \mathbf{v}} e^{w_{j,l}x_l} \right) \left(\prod_{r \notin \mathbf{v}} \epsilon(w_{j,r}) \right) \right)^2 d\mathbf{x} \\ &= \frac{1}{\text{var}(\hat{f})} \sum_{\mathbf{v}, \tilde{\mathbf{v}} \subseteq \mathbf{u}} \sum_{j,i=1}^n (-1)^{2|\mathbf{u}|-|\mathbf{v}|-|\tilde{\mathbf{v}}|} \int_{[0,1]^d} \left(\beta_j \beta_i e^{b_j+b_i} \prod_{l \in \mathbf{v}} e^{w_{j,l}x_l} \prod_{r \notin \mathbf{v}} \epsilon(w_{j,r}) \prod_{s \in \tilde{\mathbf{v}}} e^{w_{i,s}x_s} \prod_{q \notin \tilde{\mathbf{v}}} \epsilon(w_{i,q}) \right) d\mathbf{x} \\ &= \frac{1}{\text{var}(\hat{f})} \sum_{\mathbf{v}, \tilde{\mathbf{v}} \subseteq \mathbf{u}} \sum_{j,i=1}^n (-1)^{2|\mathbf{u}|-|\mathbf{v}|-|\tilde{\mathbf{v}}|} \beta_j \beta_i e^{b_j+b_i} \left(\prod_{l \in \mathbf{v} \cap \tilde{\mathbf{v}}} \epsilon(w_{j,l} + w_{i,l}) \right) \left(\prod_{r \notin \mathbf{v} \cap \tilde{\mathbf{v}}} \epsilon(w_{j,r}) \epsilon(w_{i,r}) \right). \end{aligned}$$

When we only consider the single variable case or, in other words, when $\mathbf{u} = \{k\}$, then we

arrive at equation (3.3) for the first order Sobol' indices:

$$\begin{aligned} S_k &= \frac{1}{\text{var}(\hat{f})} \sum_{j,i=1}^n \left(\beta_j \beta_i e^{b_j+b_i} \epsilon(w_{j,k} + w_{i,k}) \prod_{l \neq k} \epsilon(w_{j,l}) \epsilon(w_{i,l}) \right) - \frac{\mathbb{E}(\hat{f})^2}{\text{var}(\hat{f})} \\ &= \frac{1}{\text{var}(\hat{f})} \sum_{j,i=1}^n \beta_j \beta_i e^{b_j+b_i} (\epsilon(w_{j,k} + w_{i,k}) - \epsilon(w_{j,k}) \epsilon(w_{i,k})) \prod_{l \neq k} \epsilon(w_{j,l}) \epsilon(w_{i,l}). \end{aligned}$$

Now we derive the expressions for the total Sobol' indices for a given subset of variables of $\{x_1, \dots, x_d\}$,

$$S_{\mathbf{u}}^{\text{tot}} = 1 - \frac{\text{var}(\mathbb{E}(\hat{f}|x_r, r \notin \mathbf{u}))}{\text{var}(\hat{f})},$$

where $\mathbf{u} \subset \{1, \dots, d\}$ [20]. We find the expression for the total index $S_{\mathbf{u}}^{\text{tot}}$ for (3.2):

$$\begin{aligned} S_{\mathbf{u}}^{\text{tot}} &= 1 - \frac{1}{\text{var}(\hat{f})} \left(\int_{[0,1]^d} \left(\sum_{j=1}^n \beta_j e^{b_j} \left(\prod_{l \in \mathbf{u}} \epsilon(w_{j,l}) \right) \left(\prod_{r \notin \mathbf{u}} e^{w_{j,r} x_r} \right) \right)^2 d\mathbf{x} - \mathbb{E}(\hat{f})^2 \right) \\ &= 1 - \frac{1}{\text{var}(\hat{f})} \left(\sum_{j,i=1}^n \beta_j \beta_i e^{b_j+b_i} \left(\prod_{l \in \mathbf{u}} \epsilon(w_{j,l}) \epsilon(w_{i,l}) \right) \left(\prod_{r \notin \mathbf{u}} \epsilon(w_{j,r} + w_{i,r}) \right) - \mathbb{E}(\hat{f})^2 \right). \end{aligned}$$

When we consider the total Sobol' index corresponding to a single variable x_k , we have expression (3.4):

$$\begin{aligned} S_k^{\text{tot}} &= 1 - \frac{1}{\text{var}(\hat{f})} \left(\sum_{j,i=1}^n \beta_j \beta_i e^{b_j+b_i} \epsilon(w_{j,k}) \epsilon(w_{i,k}) \prod_{l \neq k} \epsilon(w_{j,l} + w_{i,l}) - \mathbb{E}(\hat{f})^2 \right) \\ &= 1 - \frac{1}{\text{var}(\hat{f})} \sum_{j,i=1}^n \beta_j \beta_i e^{b_j+b_i} \epsilon(w_{j,k}) \epsilon(w_{i,k}) \left(\prod_{l \neq k} \epsilon(w_{j,l} + w_{i,l}) - \prod_{r \neq k} \epsilon(w_{j,r}) \epsilon(w_{i,r}) \right). \quad \blacksquare \end{aligned}$$

Appendix B. Sobol' indices of analytic example (4.4). Here we present formulas for the analytic first order and total Sobol' indices for (4.4), given an input dimension d and parameter δ . The first order Sobol indices are the same for all $k = 1, \dots, d$. The total Sobol' indices are also the same for $k = 1, \dots, d$. The first order and total Sobol' indices are given by

$$S_k = \frac{\text{var}(\mathbb{E}(f_\delta|x_k))}{\text{var}(f_\delta)} \quad \text{and} \quad S_k^{\text{tot}} = 1 - \frac{\text{var}(\mathbb{E}(f_\delta|x_l, l \neq k))}{\text{var}(f_\delta)},$$

where

$$\begin{aligned} \text{var}(f_\delta) &= \frac{d\delta}{9} \left(\frac{3}{2} \right)^d + \delta^2 \left(\left(\frac{7}{3} \right)^d - \left(\frac{9}{4} \right)^d \right) + \frac{d}{12}, \\ \text{var}(\mathbb{E}(f_\delta|x_k)) &= \frac{\delta^2}{27} \left(\frac{9}{4} \right)^d + \frac{\delta}{9} \left(\frac{3}{2} \right)^d + \frac{1}{12}, \\ \text{var}(\mathbb{E}(f_\delta|x_l, l \neq k)) &= \frac{\delta(d-1)}{9} \left(\frac{3}{2} \right)^d + \delta^2 \left(\frac{27}{28} \left(\frac{7}{3} \right)^d - \left(\frac{9}{4} \right)^d \right) + \frac{d-1}{12}. \end{aligned}$$